DOI: http://doi.org/10.25728/cs.2021.3.8

A COMPUTER SIMULATION COMPLEX FOR ANALYSIS OF MAGNETIC GRADIOMETRY SYSTEMS

A.K. Volkovitskiy[1], A.I. Gladyshev[2], D.A. Goldin[3], E.V. Karshakov[4], B.V. Pavlov[5], and M.Yu. Tkhorenko[6]

[1, 3–5]Trapeznikov Institute of Control Sciences, Russian Academy of Sciences, Moscow, Russia
[2]Chairman, the Defense Problems Section of the Ministry of Defense under the RAS Presidium, Moscow

[1]✉avolkovitsky@yandex.ru, [2]✉ tolyagladyshev@yandex.ru, [3]✉ goldind@ipu.ru, [4]✉ karshak@mail.ru, [5]✉ pavlov@ipu.ru, [6]✉ tkhorenkom@mail.ru

Abstract. A computer simulation complex for magnetic gradiometry systems is described. This complex simulates the estimation procedure for the magnetic dipole moment of a moving object according to the magnetic gradiometry data. The paper considers the software architecture and intended purpose of the complex and the algorithms of its modules, including the magnetic field module, the ambient magnetic field module (the object's magnetic field, the main magnetic field, the magnetic anomaly, and industrial magnetic noise), and the magnetic dipole moment module. Some numerical experiments with the simulation complex are briefly described. This complex can be used to design degaussing systems for the magnetic field of moving objects.

Keywords: numerical modeling, magnetic gradiometry, degaussing.

INTRODUCTION

Several application-relevant problems require active control of the magnetic field of moving objects. Among them, we mention the following problems: (1) suppressing the effect of the carrier vehicle's field on the readings of the onboard magnetic measuring equipment during aeromagnetic survey [1] and (2) reducing the underwater vehicle's magnetic field to secure against magnetic detection means [2]. The first problem can be solved analytically when processing the received measurement information, whereas the second problem requires a special onboard degaussing system for the moving object. This system represents a set of coils with an applied current to compensate, to a certain extent, the moving object's magnetic field. Obviously, the performance of such a degaussing system strongly depends on the choice of control laws for coils currents. The paper [3] proposed an original control scheme for compensating currents based on estimating the parameters of the magnetic dipole moment (MDM) of a moving object using real-time magnetic gradiometry data from a special measuring system; the resulting MDM estimates were considered when controlling the degaussing device.

The magnetic gradiometry system can be designed in a compact form, ranging from 20 cm to 2 m, depending on the selected magnetically sensitive elements. Hence, it can be implemented on a stationary bench (like all standard means for determining the MDM currently used) and in a mobile or towed configuration. Adopting such systems, which estimate the MDM in real time during motion and can be used to control coils currents, will significantly improve the quality and reliability of degaussing of a moving object (MO). The advantages seem obvious: a closed loop control system with an MDM value feedback control is used instead of compensating the MO's magnetic field based on the static bench data. This approach considers a slow change in MO's magnetization and its magnetization reversal due to the movements of ferromagnetic masses in the Earth's magnetic field.

To assess the effectiveness of this compensation scheme when controlling the MO's magnetic field, we developed a computer simulation complex for the

magnetic gradiometry system, considering both the motion features of the MO and the measuring unit and various natural and artificial noises arising when measuring the magnetic field gradient. Thus, the complex is applied to analyze the operation of the MO's magnetic field control system. This paper describes the complex in detail.

1. STRUCTURE OF COMPUTER SIMULATION COMPLEX

The computer simulation complex for the magnetic gradiometry system is a set of software modules united in an information network that simulates the interaction of ferromagnetic objects with the Earth's magnetic field (EMF), the operation of various-type magnetic gradiometers under the motion of the object and the measuring unit, and remote determination algorithms for the MDM parameters. Simulations can be performed in real time.

Information interaction in the complex is carried out in the client-server mode. In this scheme, the central element (server) is a special software module that controls and coordinates the entire complex and writes model data to files for subsequent analysis.

In addition to the server, the complex has service modules (clients) of two fundamentally different types:

– modules implementing mathematical modeling algorithms for virtual objects, systems, and processes (virtual devices);

– user interface modules visualizing the necessary parameters and allowing the operator to manage the virtual experiment parameters in real time (indicators).

The virtual device modules include a module for determining the navigational parameters of the moving object and measuring unit, a module for calculating the magnetic field and its gradient, and a module for estimating the MDM parameters.

The composition of the indicator modules depends on the goals of the virtual experiment and can be selected individually by the operator.

The simulation mode is controlled by the system timer. Each virtual device operates independently, notifying the server about the arrival of a new data portion. In turn, the server notifies the corresponding indicators about the possibility of visualizing new data and notifies the virtual devices about the corresponding control commands received from the operator. The information generated by each virtual device is saved and processed in its data storage area; the server transfers this information to the indicator modules. During visualization, indicators and virtual devices can have a unique relationship: an indicator reflects the virtual behavior of a specific virtual device. In the general case, the data of all virtual devices are available for single visualization control. Virtual devices are always managed individually.

2. MODULE FOR DETERMININING NAVIGATIONAL PARAMETERS

This module is intended for generating data on the position, speed, and orientation of the MO and measuring unit at different time instants. Two sets of motion parameters have to be determined (for the MO and measuring unit). Therefore, the module for determining the navigational parameters consists of two parts, each generating parameters for one object (the MO or measuring unit). The operator can choose between independent and dependent laws of motion of the MO and measuring unit. The latter case is implemented if the MDM parameters are determined using a magnetic gradiometer towed behind the MO, as described in [3]. On the one hand, the simulation results can be reliably analyzed only if the navigation plan (scenario) for each computational experiment is exactly specified and strictly followed. On the other hand, the maximum degree of correspondence of the model to real physical processes is needed; particularly, the virtual MO should be controlled so that its motion matches that of the real one.

To meet these requirements, we developed a module for determining the navigational parameters in which the virtual motion is controlled according to the navigational plan (task). Moreover, motion control is largely similar to that of the ship's crew (the navigator and helmsman).

The navigational plan is a sequence of given path lines, each specified by a set of points with known geographic coordinates (latitude, longitude, and altitude), traversed by the moving object with a given linear velocity. The navigational plan is described by a structured sequence of points and saved as a text file. The navigational plan is prepared for each computational experiment separately and loaded before its start. At the same time, the operator can interactively modify the navigational plan after loading using special indicators.

In the simulation complex, the virtual object is moving along the trajectories specified by the navigational plan in two modes: manual (the operator controls the object's motion from the keyboard) and automatic (the program imitates the operator's actions).

For the convenience of virtual motion control, auxiliary control information is formed as a hint for the operator (manual mode) or a guideline for the vir-

tual autopilot (automatic mode). This control information is a scalar course deviation (correction) signal for both the operator and the autopilot. For the successful execution of the navigational task, the operator (autopilot) should maintain a motion mode in which the correction parameter is close to 0. If the object needs to deviate to the right (left) to follow the specified trajectory, then the correction value will take a positive value (a negative value, respectively). The orientation is calculated based on the parameters of the MO' s trajectory considering the sinusoidal disturbance caused by the natural waves of the marine environment. The algorithm for calculating the navigational parameters was described in detail in [4, 5].

3. MAGNETIC FIELD MODULES

Assume that the magnetic field near the moving object is induced by the following sources:

– the constant component of the MO's magnetic field caused by the "hard" (constant) magnetization of the casing materials and the operation of the onboard electrical equipment;

– the variable component of the MO' magnetic field caused by the "soft" (variable) magnetization of the casing;

– the main magnetic field;

– the short-term magnetic variation;

– the magnetic anomaly;

– industrial magnetic noise (when the magnetic measuring system is located on the coast).

The resulting magnetic field is the sum of the fields from these sources. Consider the process of calculating each of these components in detail.

When calculating the constant component of the MO's magnetic field, we assume that the MI's casing contains virtual sources of constant (hard) magnetization described by a system of local dipole transmitters in a coordinate system rigidly connected with the MO's casing. The model parameters are their magnetic dipole moments M_i and the centers' coordinates r_i. The total field has the following formula [6]:

$$B_p = \sum_i \frac{\mu_0}{4\pi} \frac{3\left(M_i^{\mathrm{T}} R_i\right) R_i - M_i R_i^2}{R_i^5}, R_i = r_i - r, \quad (1)$$

where r denotes the radius vector of the observation point. (All vectors in the paper are three-dimensional columns.)

To determine the magnetization of the ellipsoidal casing, we emphasize that the magnetic field induced by the shell can be written as a gradient of some scalar potential [7]:

$$B_s = -\nabla u. \quad (3)$$

It can be shown that the scalar function u introduced in this way satisfies the Laplace equation both inside the casing and outside it. Moreover, the boundary conditions for Maxwell's equations hold on the casing surfaces. Hence, the solution functions u_1 (outside the casing), u_2 (in the casing walls) and u_3 (inside the casing) are given by [8]:

$$\begin{aligned} u_1 &= \sum_{n=0}^{\infty} \sum_{m=-n}^{n} D_{nm} Q_n^m(\eta) Y_n^m(\theta,\phi), \\ u_2 &= \sum_{n=0}^{\infty} \sum_{m=-n}^{n} \left(B_{nm} Q_n^m(\eta) + C_{nm} P_n^m(\eta)\right) \times \\ &\quad \times Y_n^m(\theta,\phi), \\ u_3 &= \sum_{n=0}^{\infty} \sum_{m=-n}^{n} A_{nm} P_n^m(\eta) Y_n^m(\theta,\phi), \end{aligned} \quad (4)$$

where n is the maximum order of the expansion; $\eta, \theta,$ and ϕ are the prolate spheroidal coordinates; $P_n^m(\eta)$ and $Q_n^m(\eta)$ are the associated Legendre functions of the first and second kinds, respectively; finally, $Y_n^m(\theta,\phi)$ are the spherical functions [9]. The constants $A_{nm}, B_{nm}, C_{nm},$ and D_{nm} are obtained from the system of linear equations

$$\begin{aligned} B_{nm} Q_n^m(\eta) + (C_{nm} - A_{nm}) P_n^m(\eta) &= 0, \eta = \eta_2, \\ (B_{nm} - D_{nm}) Q_n^m(\eta) + C_{nm} P_n^m(\eta) &= u_{nm}, \eta = \eta_1, \\ \mu B_{nm} Q'^m_n(\eta) + (\mu C_{nm} - \mu_0 A_{nm}) P'^m_n(\eta) &= 0, \eta = \eta_2, \\ (\mu B_{nm} - \mu_0 D_{nm}) Q'^m_n(\eta) + \mu C_{nm} P'^m_n(\eta) &= \\ = \mu_0 w_{nm}, \eta &= \eta_1, \end{aligned} \quad (5)$$

where η_1 and η_2 are the geometrical parameters determining the outer and inner ellipsoidal surfaces, and the coefficients u_{nm} and w_{nm} are given by

$$\begin{aligned} u_{nm} &= \frac{1}{\| Y_n^m \|^2} \int_0^{2\pi} d\phi \int_0^{\pi} d\theta \sin\theta u_e(\eta,\theta,\phi) Y_n^m(\theta,\phi), \\ w_{nm} &= \frac{1}{\| Y_n^m \|^2} \int_0^{2\pi} d\phi \int_0^{\pi} d\theta \sin\theta \frac{\partial u_e(\eta,\theta,\phi)}{\partial \eta} Y_n^m(\theta,\phi), \end{aligned} \quad (6)$$

where u_e is the scalar potential of external sources (the EMF, the magnetic field of the system of constant dipoles). In the simulation complex, the integrals (6) can be calculated in two ways: using the Gauss–Legendre quadrature method [10] and a generalization of the sampling theorem [11]. With the coefficients $A_{nm}, B_{nm}, C_{nm},$ and D_{nm} obtained from (5), the scalar potential and the magnetic field can be calculated by formulas (4) and (3). Thus, the magnetic field of the casing can be expanded into a series with respect to the spherical functions: the input parameters are the geometric dimensions of the casing and the magnetic permeability of its material, and the expansion coeffi-

cients depend on the EMF. They are recalculated at each step of the algorithm.

In this complex, the main magnetic field is calculated using the IGRF 13 model [12]. Similar to the casing field, the main magnetic field is written as the gradient of the scalar potential given by

$$u = a\sum_{n=1}^{N}\sum_{m=0}^{n}\left(\frac{a}{r}\right)^{n+1}(g_{mn}\cos m\phi + h_{mn}\sin m\phi)\times \\ \times P_n^m(\cos\theta), \quad (7)$$

$$g_{mn} = g_{mn}^0 + \dot{g}_{mn}(t-t_0),$$

$$h_{mn} = h_{mn}^0 + \dot{h}_{mn}(t-t_0),$$

where $r, \theta,$ and ϕ are the spherical coordinates of the observation point, and t denotes time. The components of the magnetic induction vector are calculated by formula (3). The constants $a, t_0, g_{mn}^0, \dot{g}_{mn}, h_{mn},$ and $\dot{h}_{mn}$ are known and loaded from the file before the operation starts.

The short-term magnetic variation is written as the sum of sinusoidal components

$$B_v = \sum_i \left(C_i\cos\omega_i t + S_i\sin\omega_i t\right). \quad (8)$$

The values $C_i, S_i,$ and ω_i are input parameters specified in the settings file.

The magnetic anomaly is described by a synthetic model built as the potential of dipoles randomly distributed in a square of 10×10 km, with a periodically repeating palette. During the simulation, the depth of the dipoles' layer is set to 1 km; the range of the maximum dipole moment amplitude, to ± 25 MA · m^2. The anomaly field does not reflect the true structure of the EMF of the indicated area, just simulating the characteristic magnetic disturbances and inhomogeneities in the magnetization of geological structures. Nevertheless, the model has an adequate behavior: as the height increases (deep water), the amplitude of anomalies decreases, and the characteristic period increases. The total field of anomalies is calculated using a formula similar to (1). The correspondence of the magnetic anomaly model to the true magnetic field distribution is not significant for the algorithm for determining the MDM: the very presence or absence of an anomalous component affecting the operation of this algorithm is essential. The synthetic magnetic anomaly model allows estimating this effect in the simulation mode and establishing the conditions under which the remote determination of the MDM during sailing can be considered correct. The model does not evolve, being stable over time. The model parameters are "hardly" embedded into the program code of the only available function. Calling this function generates the parameters of the model field.

Finally, the industrial noise is simulated using the field of a system of infinitely thin wires with a sinusoidal current of industrial frequency (50 Hz or 60 Hz) applied. The magnetic field of a wire with an applied current has a simple analytical expression [6]: the total wire field is simply the vector sum of the individual wire fields. The input data for simulation are the geometric parameters of the system and the frequency and amplitude of the wires currents.

4. MAGNETIC DIPOLE MOMENT MODULE

This module simulates the process of magnetic measurements and determines the MDM by these measurements. First, we describe the simulation of measurements.

The complex simulates the operation of the measuring unit with a spaced layout of the sensors (Fig. 1). The virtual unit represents a regular tetrahedral pyramid with magnetic sensors *S*1–*S*4. In addition, the unit includes blocks of an orientation system (indicated by GIS) to determine the spatial and angular position.

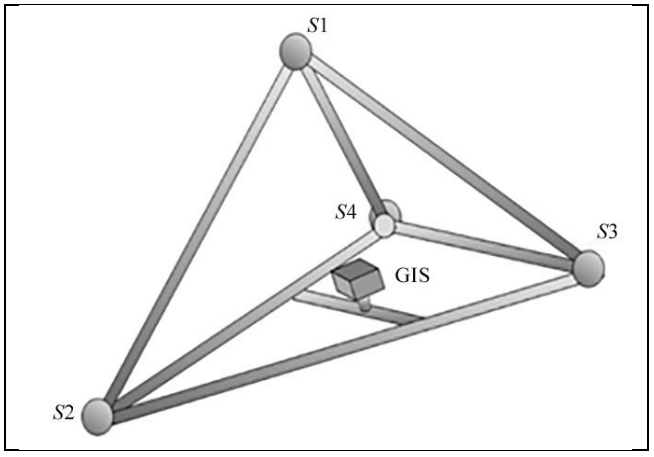

Fig. 1. Magnetosensitive measuring unit on spaced sensors.

The complex simulates the operation of the measuring unit using magnetic sensors of three different types:

– scalar sensors (quantum sensors) [13],

– vector three-component sensors of high sensitivity and accuracy (superconducting quantum interference devices, SQUIDs) [14],

– vector three-component sensors of low sensitivity and accuracy (fluxgate magnetometers) [13].

The first type corresponds to a vector magnetic gradiometer; the second and third ones, to a tensor magnetic gradiometer.

The operation of magnetosensitive elements of all three types is simulated by the same scheme. At each

cycle of the system time, the following actions are performed:

- The model ("true") parameters of the position—coordinates and orientation—are calculated for each sensor of the virtual magnetic measuring unit using the procedures of the navigation module of the measuring unit.
- The new ("distorted") values of the spatial coordinates of the measuring units are calculated. (The deformation of the magnetic gradiometer unit's platform is simulated.)
- The components of the model ("true") magnetic field vector are calculated for the "distorted" position parameters in the coordinate system associated with each sensor.
- The parameters of the "true" field vector are virtually measured in accordance with the model parameters of the sensor's measuring properties: the parameters of the new "measured" field vector, distorted relative to the "true" one, are calculated. The distortions result from the systematic zero-drift errors, deviations from the scale factor from 1 (for each component of the vector), the non-orthogonality of the sensitive axes, and measurement noises.
- If the scenario assumes simulating the measuring unit using scalar magnetosensitive elements, then for each sensor, the "measured" vector parameters are transformed to scalars by taking the absolute value.
- Depending on the type of sensors, the type of the magnetic gradiometer unit is automatically determined: the unit will "measure" the gradient vector of the field's absolute value in the case of scalar sensors and the tensor of the second derivative of the field potential in the case of vector sensors.
- The orientation angles of the "true" position parameters block are also measured virtually: the "measured" parameters of the angular orientation vector are calculated. They differ from the "true" ones due to the systematic distortions under the specified accuracy parameters of the virtual orientation system of the measuring unit.

The calculated "measured" parameters are input data for the algorithm for determining the MDM parameters.

Note that this module may operate in the calibration and measurement modes. The former mode activates the algorithm for calculating the corrections for the virtual measurement data. The corrections are introduced by "measuring" the alternating field induced by the virtual reference source. The difference between the measurement and calibration modes is the absence of the reference field: during virtual measurements, the reference field source is switched off.

Let us briefly describe the algorithm for estimating the MDM parameters by magnetic field measurements. For the sake of definiteness, consider a tensor measuring unit. Assume that a single dipole is located at the origin of the coordinate system. Then formula (1) yields

$$B = \frac{\mu_0}{4\pi r^5}\left(3rr^{\mathrm{T}} - r^2 I\right)M. \qquad (9)$$

Here M is the magnetic dipole moment; I denotes an identity matrix of dimensions 3×3; rr^{T} is the outer product of the vectors. We will determine r and M by the known values of the left-hand side of (9) at several measurement points and the distance between them. For each of 4 vector field sensors, we calculate

$$B_i = \frac{\mu\mu_0}{4\pi\left|\tilde{r} + \delta r_i\right|^3}\left(3\frac{\left(\tilde{r} + \delta r_i\right)\left(\tilde{r} + \delta r_i\right)^{\mathrm{T}}}{\left(\tilde{r} + \delta r_i\right)^{T}\left(\tilde{r} + \delta r_i\right)} - I\right)\tilde{M}. \qquad (10)$$

Here $\tilde{M}$ and $\tilde{r}$ are the estimates of M and r; δr_i are the known displacement vectors of the vector magnetic sensors relative to the system's measuring center; B_i is the calculated value of the field vector under the current hypothesis for sensor i.

Since the field vector measurements are subject to variations, we should consider the differences in the field components. The magnetic field variations are spatially homogeneous enough to neglect their spatial variations at distances of up to several kilometers.

We introduce the vector of estimated parameters

$$x = \left(r_1, r_2, r_3, m_1, m_2, m_3\right),$$

where r_i are the components of the corrections vector for some prior estimate of the radius vector r of the dipole location point; m_i are the components of the corrections vector for some prior estimate of the dipole moment vector M:

$$X = X_0 + x, X_0 = \left(\tilde{r}_1, \tilde{r}_2, \tilde{r}_3, \tilde{M}_1, \tilde{M}_2, \tilde{M}_3\right).$$

Next, we introduce the vector of the measured componentwise differences between the vector sensors readings:

$$z = \left(z_{121}, z_{122}, z_{123}, z_{231}, z_{232}, z_{233}, z_{241}, z_{242}, z_{243}\right).$$

Here the first subscript corresponds to the number of the "minuend" sensor; the second subscript, to the number of the "subtrahend" sensor; the third subscript, to the number of the sensitivity axis along which the difference is measured. Despite that 18 such differences are measured for 4 sensors in total, only 9 of them can be considered independent: any other component of the differences can be expressed through the parameters of the vector z. Now we introduce a vector containing the parameters of the gradient (the differences of the field components):

$$G = \left(G_{121}, G_{122}, G_{123}, G_{231}, G_{232}, G_{233}, G_{241}, G_{242}, G_{243}\right),$$
$$G_{ijk} = B_{ik} - B_{jk}.$$

Note that G_{ijk} are expressed through r and M using formula (10). Thus, the problem is finding r and M satisfying the relations

$$G_{ijk} = f_{ijk}\left(r, M\right),$$

where f_{ijk} are nonlinear functions of r and M, expressed through formula (10). This class of problems can be solved using a nonlinear generalization of the Kalman filter—the Iterated Extended Kalman Filter (IEKF) [15–18].

A similar approach applies to determining the MDM parameters by the gradient vector measurements. The only difference is that the measurements equation will include not the differences between the field vectors components but the differences between their absolute values. However, in the configuration of the measuring system with 4 sensors, a vector gradiometer yields 3 independent measurements: we can determine only the MDM parameters but not the MDM radius vector.

Numerical experiments show that under moderate errors in the prior estimates of r and M and measurement noises, this algorithm always converges to the true values of the MDM parameters. Its domain of convergence is presented in Fig. 2. The corresponding initial conditions are from a cube of dimensions 40 × 40 × 40 m (from –20 to +20 for each coordinate), and the dipole position is (5, 0, 0.306). The dipole moment is equal to 100 Am^2, and the measurement noise of the field components is nT. The shade of gray indicates the number of iterations for reaching the solution point. Due to the gradiometer's design, the plane passing through its center (with the normal directed to the dipole) is the boundary of this domain; see Fig. 2.

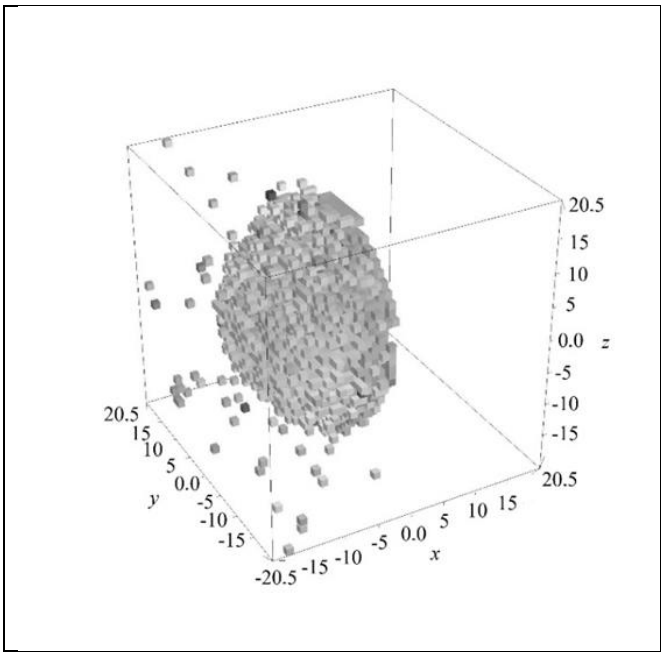

Fig. 2. The domain of convergence for iterative algorithm.

5. EXAMPLES OF NUMERICAL EXPERIMENTS WITH THE SIMULATION COMPLEX

To demonstrate the effectiveness of the algorithms for determining the MDM by the magnetic field gradient parameters at the detector's location, we carried out several numerical experiments with the simulation complex. The results of some experiments are presented below. To control the accuracy of determining the MDM by the detector, we applied the following approach: given the parameters of the object's model, we calculated the asymptotic behavior of the magnetic field at infinity, corresponding to the field of a point magnetic dipole (decreasing no faster than $1/r^3$). Note that the main magnetic field, the magnetic anomaly, and industrial noise were not included in the model field expression.

The first experiment simulated the simplest possible situation: the object's motion with a detector towed behind it on a flexible cable along a rectilinear route. The field of a point magnetic dipole was the object's field, and the fields of magnetic anomaly and industrial noise were neglected. The results of this experiment are shown in Figs. 3–5. (All values on the right scale of Fig. 5 are multiplied by 10^6.)

Clearly, the algorithm for calculating the MDM converges rather quickly to the true dipole moment value (the coefficient at the expansion term decreasing with a rate of $1/r^3$).

The second experiment simulated the estimation procedure of the MDM considering the sensors' noises and the inaccurately known geometry of the measuring unit. The results are shown in Figs. 6–8. (All values on the right scale of Fig. 8 are multiplied by 10^6.) This experiment was carried out with the following mean-squared errors of the geometric parameters: 10 cm (the distance between the object and detector), 2 mm (the distance between the individual sensors in the detector, with a sensor spacing of 2 m), and 10^{-4} rad (the orientation of the sensitivity axes of the magnetic measuring system). Quite expectedly, the estimation quality decreased compared to the first experiment.

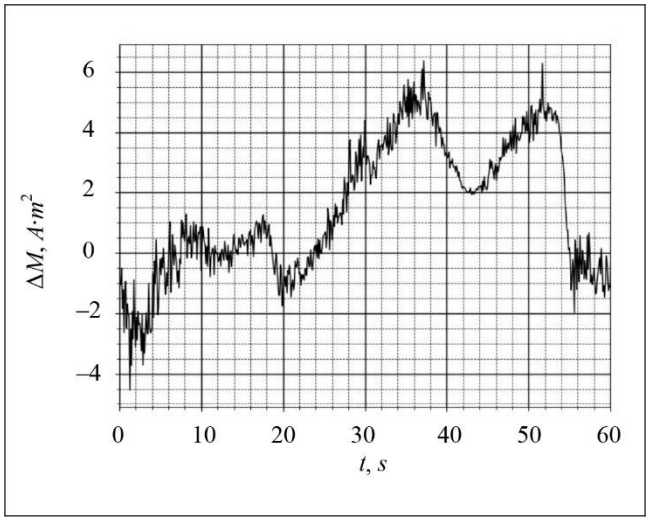

Fig. 3. Estimation error for the absolute value of MDM.

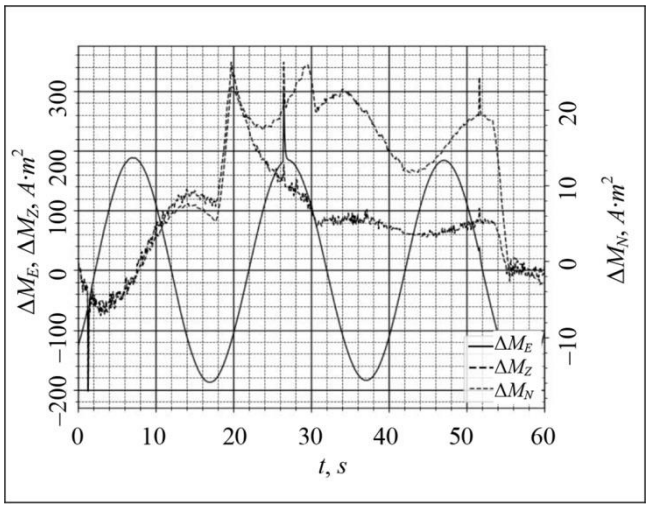

Fig. 4. Estimation errors for MDM components.

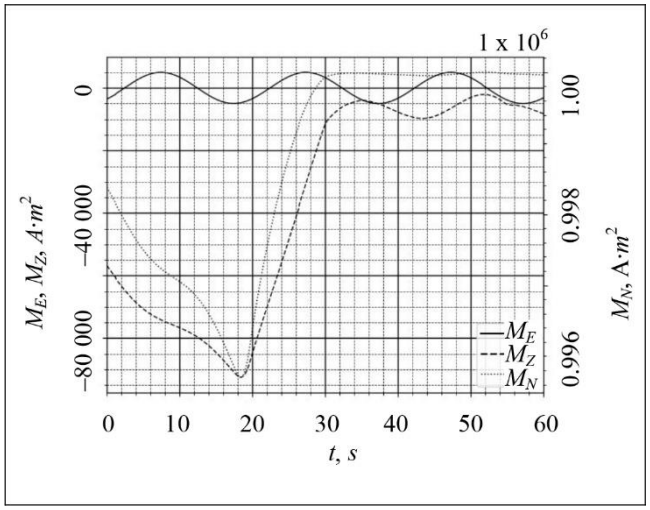

Fig. 5. MDM components.

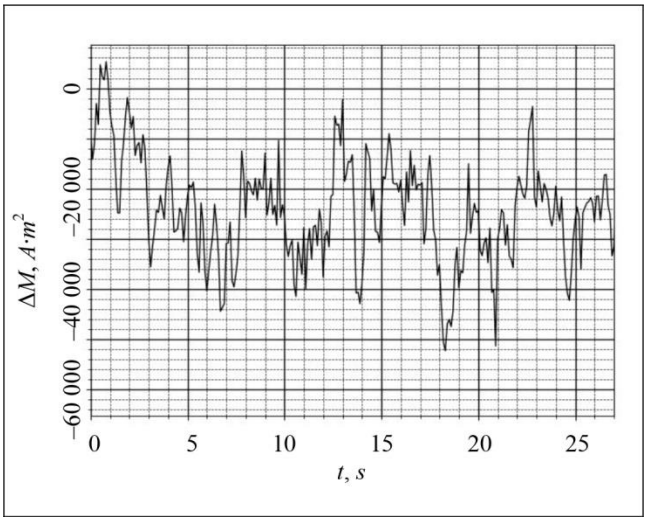

Fig. 6. Estimation error for the absolute value of MDM.

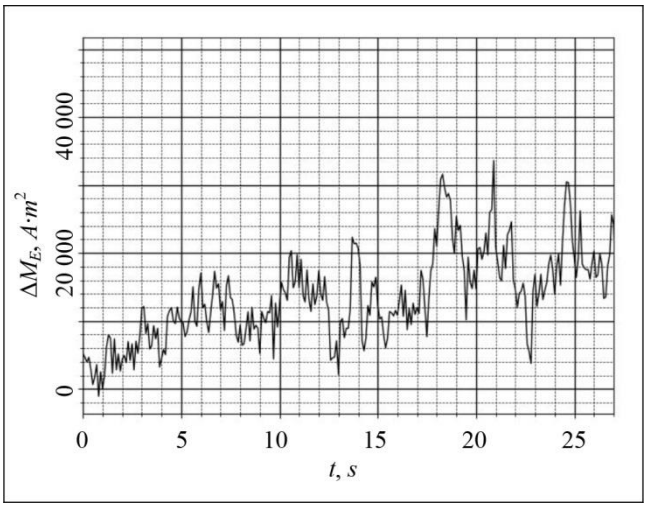

Fig. 7. Estimation error for MDM component.

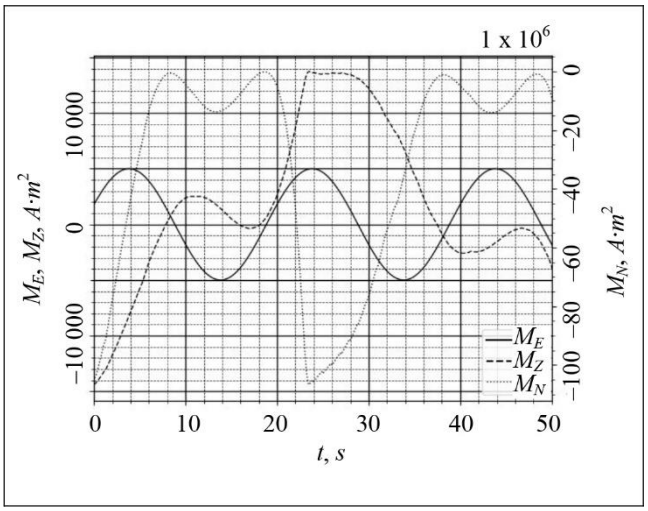

Fig. 8. MDM components.

In the third experiment, we calculated the object's magnetic field as the sum of the fields induced by a system of point dipoles and a homogeneous casing. The results of this experiment are shown in Figs. 9–11. (All values on the right and left scales of Fig. 11 are multiplied by 10^6.) The quality of estimating the MDM is worse than in the first experiment. This fact is explained both by the algorithm's peculiarities (it is based on the point dipole field formula and determines the MDM of more complex systems only approximately) and by the presence of the simulated measurement noises. Moreover, it was assumed that the object was moving along a curved route with maneuvering. Note that the estimation errors in the third experiment are not much worse than in the second experiment. Therefore, the algorithms under consideration are applicable for estimating the MDM of the objects with a rather complex structure of their magnetic field.

CONCLUSIONS

This paper has considered a computer complex developed by the authors to simulate the operation of a magnetic gradiometry system in the process of estimating the MO's MDM. The general structure and principles of the complex and the purpose of individual service modules have been described in detail. In addition, three algorithms have been presented: an algorithm for simulating the MO's magnetic field that includes two components (the constant field and the field of an ellipsoidal casing), an algorithm for simulating the main magnetic field and various noises (the industrial noises, the magnetic anomaly, and the short-term magnetic variation), and a nonlinear algorithm for estimating the MDM parameters by measurements of the magnetic field vector components at several points with fixed spacing. Finally, several numerical experiments with the simulation complex have been provided.

The complex estimates the MO's MDM in the stationary, mobile, and towed configurations. The complex can be used to assess the effectiveness of implementing the described MDM estimation systems in real time during motion and test coil current control during the degaussing of the MO, which may significantly improve its quality and reliability.

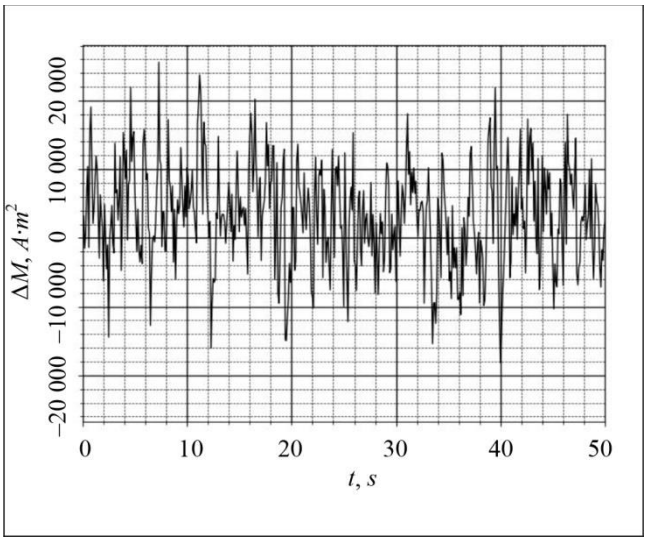

Fig. 9. Estimation error for the absolute value of MDM.

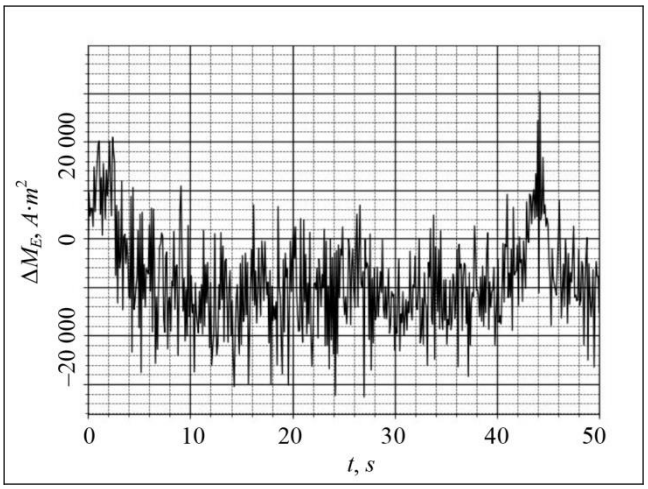

Fig. 10. Estimation error for MDM component.

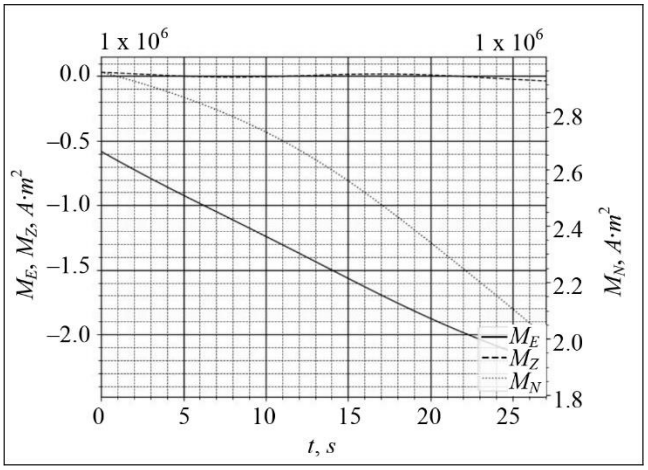

Fig. 11. MDM components.

REFERENCES

1. Noriega, G., Aeromagnetic Compensation in Gradiometry – Performance, Model Stability, and Robustness, *IEEE Geoscience and Remote Sensing Letters*, 2015, vol. 12, iss. 1, pp. 117–121.
2. Bayens, T.M., Analysis of the Demagnetisation Process and Possible Alternative Magnetic Treatments for Naval Vessels, *PhD Dissertation*, Sydney: University of New South Wales, 2002.
3. Volkovitskiy, A.K., Karshakov, E.V., Tkhorenko, M.Yu., and Pavlov, B.V. Application of Magnetic Gradiometers to Control Magnetic Field of a Moving Object, *Automation and Remote Control*, 2020, no. 2, vol. 81, pp. 333-339.
4. Volkovitsky, A.K., Karshakov, E.V., and Pavlov, B.V., The Structure of the Control Algorithms of Aircraft Navigating, *Izv. SFedU. Engineering Sciences*, 2013, no. 3 (140), pp. 217–225. (In Russian.)
5. Karshakov, E.V., Shevchenko, A.M., and Garakoev, A.M., Formation of a Director Index to Assist the Pilot in Conducting Airborne Geophysical Survey, *IOP Conference Series: Materials Science and Engineering - International Workshop on Navigation and Motion Control* (*NMC 2020*), 2020, vol. 984, p. 012015 (1-10).
6. Purcell, E., *Electricity and Magnetism*, 3rd. ed., Cambridge: Cambridge Univ. Press, 2013.
7. 7. Landau, L.D., Lifshitz, E.M., and Pitaevskii, L.P., *Course of Theoretical Physics. Vol. 8: Electrodynamics of Continuous Media*, 2nd ed., Butterworth-Heinemann, 1984.
8. Moon, P. and Spencer, D.E., *Field Theory Handbook*, Springer-Verlag, 1988.
9. Abramowitz, M. and Stegun, I.A., *Handbook of Mathematical Functions with Formulas, Graphs and Mathematical Tables*, National Bureau of Standards, 1964.
10. Press, W.H., Teukolsky, S.A., Vetterling, W.T., and Flannery, B.P., *Numerical Recipes: The Art of Scientific Computing*, Cambridge: Cambridge University Press, 2007.
11. Dricsoll, J.R. and Healy, D.M., Computing Fourier Transforms and Convolutions on 2-Sphere, *Advances in Applied Mathematics*, 1994, vol. 15, pp. 202–250.
12. Thebault, E., Finlay, C.C., Beggan, C.D., et al., International Geomagnetic Reference Field: the 12th Generation, *Earth, Planets and Space*, 2015, vol. 67, article no. 79, pp. 1–19.
13. Telford, W.M., Geldart, L.R. and Sherif, R.E., *Applied Geophysics*, Cambridge: Cambridge University Press, 2004.
14. Foley, C.P., Tilbrook, D.L., Leslie, K.E., et al., Geophysical Exploration Using Magnetic Gradiometry Based on HTS SQUIDs, *IEEE Trans. Appl. Superconductivity*, 2001, vol. 11, no. 1, pp. 1375–1378.
15. *Handbook of Applicable Mathematics. Vol. 6: Statistics*, Ledermann, W. and Lloyd, E., Eds., Wiley, 1984.
16. Stepanov, O.A., *Primenenie teorii nelineinoi fil'tratsii v zadachakh obrabotki navigatsionnoi informatsii* (Application of Nonlinear Filtering in Navigational Data Processing), St. Petersburg: Concern CSRI Elektropribor, 2003. (In Russian.)
17. Simon, D., *Optimal State Estimation. Kalman, H_∞ and Nonlinear Approaches*, Wiley, 2006.
18. Xu, Y., Chen, X., and Li, Q., Adaptive Iterated Extended Kalman Filter and Its Application to Autonomous Integrated Navigation for Indoor Robot, *The Scientific World Journal*, 2014, vol. 2014, p. 7.

This paper was recommended for publication by L.B. Rapoport, a member of the Editorial Board.

Received April 7, 2021, and revised April 22, 2021. Accepted May 13, 2021.

Author information

Volkovitskiy, Andrei Kirillovich. Senior researcher, Trapeznikov Institute of Control Sciences, Russian Academy of Sciences, Moscow, Russia, ✉ avolkovitsky@yandex.ru

Gladyshev, Anatoly Ivanovich. Chairman, the Defense Problems Section of the Ministry of Defense under the RAS Presidium, Moscow, Russia, ✉ tolyagladyshev@yandex.ru

Goldin, Dmitry Alekseevich. Senior researcher, Trapeznikov Institute of Control Sciences, Russian Academy of Sciences, Moscow, Russia, ✉ goldind@ipu.ru

Karshakov, Evgeny Vladimirovich. Leading researcher, Trapeznikov Institute of Control Sciences, Russian Academy of Sciences, Moscow, Russia, ✉ karshakov@ipu.ru

Pavlov, Boris Viktorovich. Chief researcher, Trapeznikov Institute of Control Sciences, Russian Academy of Sciences, Moscow, Russia, ✉ pavlov@ipu.ru

Tkhorenko, Maksim Yur'evich. Senior researcher, Trapeznikov Institute of Control Sciences, Russian Academy of Sciences, Moscow, Russia, ✉ tkhorenkom@mail.ru

Cite this article

Volkovitskiy, A.K., Gladyshev, A.I., Goldin, D.A., Karshakov, E.V., Pavlov, B.V., Tkhorenko, M.Yu. A Computer Simulation Complex for Analysis of Magnetic Gradiometry Systems. *Control Sciences* **3,** 57–65 (2021). http://doi.org/10.25728/cs.2021.3.8

Original Russian Text © Volkovitskiy, A.K., Gladyshev, A.I., Goldin, D.A., Karshakov, E.V., Pavlov, B.V., Tkhorenko, M.Yu., 2021, published in *Problemy Upravleniya*, 2021, no. 3, pp. 65–74.